Michigan State University

National Superconducting Cyclotron Laboratory

IMAGING OF SOURCES IN HEAVY-ION REACTIONS

D.A. BROWN and PAWEL DANIELEWICZ

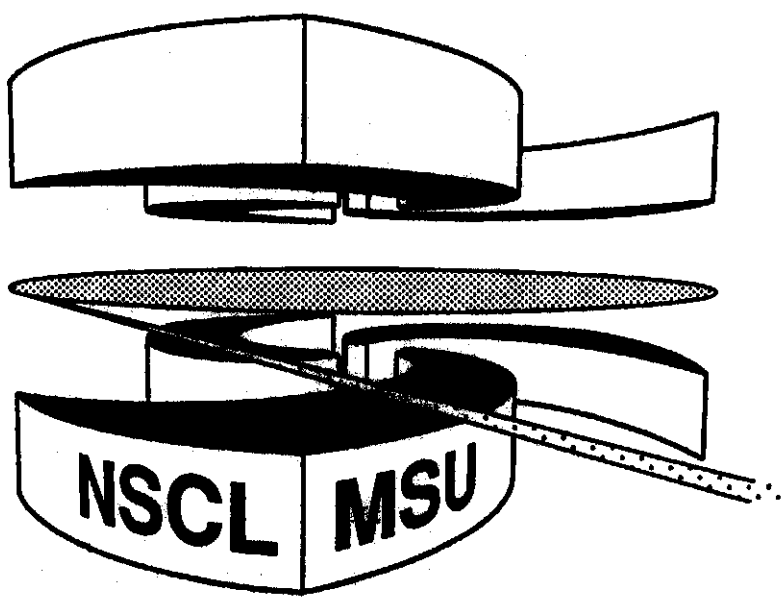

MSUCL-1054

JANUARY 1997

MSUCL-1054

Imaging of Sources in Heavy-Ion Reactions

David A. Brown' and Paweł Danielewicz†

National Superconducting Cyclotron Laboratory and

Department of Physics and Astronomy, Michigan State University,

East Lansing, Michigan *48824, USA*

(January 27, 1997)

Abstract

Imaging of sources from data within the intensity interferometry is discussed. In the two-pion case, the relative pion source function may be determined through the Fourier transformation of the correlation function. In the proton-proton case, the discretized source function may be fitted to the correlation data.

PACS numbers: 25.75.Gz, 25.75.-q

'e-mail: dbrown@nscl.msu.edu

†e-mail: danielewicz@nscl.msu.edu

Phase interferometry [1] has been shown to be capable of delivering star images in astronomy, e.g. that of Betelgeuse [2]. Intensity interferometry, such as is applied in nuclear physics, has been primarily used to determine radii of stars in astronomy and of particle emitting regions in the heavy-ion reactions. In heavy-ion reactions, this determination has been done, most often, by fitting the low-momentum two-particle correlation functions under an assumption of Gaussian-shaped emitting regions [3]. Source lifetimes have been inferred in the reactions by considering a similarly-shaped distribution of emission times. However, it was not always clear that the analyzed data could truly narrow down the lifetimes for short-lived sources. Bertsch [4] noted that an integral over the low-momentum correlation function can yield the value of the source function at the zero relative distance. Beyond this, no attempts were made to image the source function from the reaction data. Typically, comparisons to reaction simulations have been carried out by generating the correlation functions from simulated events.

In this letter we investigate the feasibility of direct imaging of the source from the reaction data, within the intensity interferometry. Given a two-particle correlation function, this represents an inversion problem. Two examples are considered, that of like-charged-pion and that of proton-proton interferometry. In the like-pion case, the relative source function results as a Fourier transformation of the two-particle correlation. In the proton case, the procedure is more involved. In this letter, we first discuss the relation of the correlation function to the source function, then the imaging, and finally some informational content in the images.

Under the assumptions of the approximate independence of processes leading to two particles in the final state and of the weak dependence of the product of single-particle sources $\overline{D}$ on momenta important for correlations, the two-particle correlation function may be represented as [5,6]

$$C_{\mathbf{P}}(\mathbf{q}) = \frac{dN_2/d\mathbf{p}_1\, d\mathbf{p}_2}{(dN_1/d\mathbf{p}_1)\,(dN_1/d\mathbf{p}_2)} \simeq \int d\mathbf{r}\, |\Phi_{\mathbf{q}}^{(-)}(\mathbf{r})|^2\, S_{\mathbf{P}}(\mathbf{r}), \qquad (1)$$

where

$$S_{\mathbf{P}}(\mathbf{r}) = \int d\mathbf{R}\, dt_1\, dt_2\, \overline{D}(0, \mathbf{R} + \mathbf{r}/2, t_1)\, \overline{D}(0, \mathbf{R} - \mathbf{r}/2, t_2)\,. \tag{2}$$

The momentum $\mathbf{P}$ above is the total momentum of a pair and $\mathbf{q}$ is the cm relative momentum. The integrations in the last expression in (1) and on the r.h.s. of (2) are over cm variables; the single-particles sources, $\overline{D} = D / \int d\mathbf{r}\, dt\, D$, are taken in the pair cm frame. The function D is the distribution of last collisions for an emitted particle in space, time, and momentum. For Klein-Gordon fields, with $(\Box + m_\pi^2)\phi(x) = -j(x)$, D may be written, in terms of single-particle self-energies, as

$$D(\mathbf{p}, \mathbf{r}, t) = \frac{i}{2E_p}\, \Pi^<(\mathbf{p}, E_p, \mathbf{r}, t) \exp\left[-\frac{1}{2E_p} \int_t^\infty dt'\, (-2)\mathrm{Im}\, \Pi^+\, (\mathbf{p}, E_p, \mathbf{r} + v_{\mathbf{p}}(t' - t), t')\right], \tag{3}$$

where $i\Pi^<(x, x') = \langle j(x')\, j(x)\rangle_{\text{irred}}$, and $(-2)\mathrm{Im}\, \Pi^+(x, x') = \langle [j(x), j(x')]\rangle_{\text{irred}}$. For the Schrödinger fields, with $\left(i\frac{\partial}{\partial t} + \frac{\nabla^2}{2m}\right) \Psi(x) = j(x)$, the analogous result is

$$D(\mathbf{p}, \mathbf{r}, t) = \mp i\Sigma^<(\mathbf{p}, E_{\mathbf{p}}, \mathbf{r}, t) \exp\left[-\int_t^\infty dt'\, \Gamma\, (\mathbf{p}, E_{\mathbf{p}}, \mathbf{r} + v_{\mathbf{p}}(t' - t), t')\right], \tag{4}$$

where $\mp i\Sigma^<$ is the single-particle production rate, $\mp i\Sigma^<(x, x') = \langle j(x')\, j(x)\rangle_{\text{irred}}$, and Γ is the damping rate. For particles with spin, the modulus of the wavefunction in (1) should be averaged over spin directions. Deviations from (2), for low r within the source, could be expected in the presence of short-range repulsion. The results (1), (3), and (4) ignore the final-state refraction. The effects of the Coulomb field of a source are discussed in a separate paper [7]. For pion-pion correlations these effects may be approximately removed directly from the correlation function [8], just as with the effects of the pion-pion Coulomb interaction.

While, with the formulas above, the correlation function C has an *indirect* dependence on other quantities, it is directly shaped by S in the reaction, i.e. by the relative distribution of emission points for two particles with similar momenta, in their center of mass. With (2), S is normalized to 1, as $\overline{D}$ is normalized to 1. For like particles, S is a symmetric function; this would not be generally the case for distinct particles. Depending on the circumstances in a reaction, S may range from isotropic, for prompt emission, to strongly elongated along $\mathbf{P}$,

and possibly even bone-shaped, for emission from a long-lived source. The transverse size, in the last case, would be close to the size of a nucleus at short longitudinal distances and widen at larger distances due to the zigzaging of the source under the recoil caused by emission. The lifetime might be read off from the elongation of S.

With (1), the goal of the imaging is the determination of S given C. Given that the interesting part of C is its deviation from 1, we may subtract 1 from both sides of (1) obtaining

$$C_{\mathbf{P}}(\mathbf{q}) - 1 = \int d\mathbf{r} \left(|\Phi_{\mathbf{q}}^{(-)}(\mathbf{r})|^2 - 1 \right) S_{\mathbf{P}}(\mathbf{r}) = \int d\mathbf{r}\, K(\mathbf{q},\mathbf{r})\, S_{\mathbf{P}}(\mathbf{r}), \tag{5}$$

where $K = |\Phi_{\mathbf{q}}^{(-)}|^2 - 1$. The problem of imaging then reduces to the inversion of K. A difficulty may arise from the presence of a kernel (or null-space) of K, i.e. the subspace of functions that the operator K turns to zero. The projection of S onto the kernel cannot then be restored within imaging. It will become apparent that, in the case of like particles, the kernel of K is empty. For unlike particles, when one of the particles is neutral, the imaging may not be able to restore portions of S for large particle separations as K approaches zero for large separations; a particular severe situation occurs for $|\Phi_{\mathbf{q}}^{(-)}|^2 \simeq 1$, when the whole space of functions becomes the kernel.

When ignoring interactions for like-pion pairs, Eq. (5) may be written as

$$C_{\mathbf{P}}(\mathbf{q}) - 1 = \int d\mathbf{r} \cos(2\mathbf{q}\mathbf{r})\, S_{\mathbf{P}}(\mathbf{r}). \tag{6}$$

Given that S is symmetric, the Fourier transform can be inverted to yield

$$S_{\mathbf{P}}(\mathbf{r}) = \frac{1}{\pi^3} \int d\mathbf{q} \cos(2\mathbf{q}\mathbf{r}) \left(C_{\mathbf{P}}(\mathbf{q}) - 1 \right). \tag{7}$$

The directions that may be used in the analysis of S correspond to those commonly employed for sources in the overall frame: outward along the transverse momentum of the pair, longitudinal along the beam, and the remaining direction, termed transverse. Equation (7) has important implications for the angular moments of the source and the correlation function. If we introduce $C(\mathbf{q}) = \sqrt{4\pi} \sum_{\ell m} C^{\ell m}(q)\, \mathrm{Y}^{\ell m}(\Omega_{\mathbf{q}})$ and an analogous representation for S, then, from (7), we get the relation

$$S_{\mathbf{P}}^{\ell m}(r) = \frac{(-1)^{\ell/2}\, 4}{\pi^2} \int_0^\infty dq\, q^2\, j_\ell(2qr)\, (C_{\mathbf{P}}^{\ell m}(r) - \delta^{\ell 0}\, \delta^{m 0})\,. \tag{8}$$

Due to the symmetry of S and C, only even ℓ appear in the angular expansion of these functions. Since both functions are real, the moments satisfy $(C^{\ell m})^* = (-1)^m\, C^{\ell -m}$. The relation (8) between the angular moments may help in analyzing the three-dimensional data. The relation shows, in particular, that the angle-averaged correlation function $C^{00}(q) \equiv C(q)$ reflects the angle-averaged source $S^{00}(r) \equiv S(r)$,

$$r\, S_{\mathbf{P}}(r) = \frac{2}{\pi^2} \int_0^\infty dq\, q\, \sin(2qr)\, (C_{\mathbf{P}}(q) - 1)\,. \tag{9}$$

As a specific example of the source extraction, we present in Fig. 1 the relative angle-averaged π^- source-function determined, using Eq. (9), from the central 10.8 GeV/c Au + Au data of Ref. [9]. Prior to the Fourier transformation in (9), the data were corrected for the Coulomb interaction between the two pions and between the pions and the source [8], with the latter interaction causing refraction. The integration in (9) for Fig. 1 has been carried out up to $q_{\mathbf{max}} \simeq 50$ MeV/c which gives a resolution in the relative distance in the figure of $\Delta r \sim 1/2q_{\mathbf{max}} \sim 2.0$ fm. The largest r that may be considered follows from $1/2\,\Delta q$, where Δq is the momentum resolution for the data ($\Delta q = 5$ MeV/c in the case of [9]).

Also in the general case, the respective angular moments of C and S are directly related. Thus, the spin-averaged operator K depends only on the angle between $\mathbf{q}$ and $\mathbf{r}$, and not on the separate directions of these vectors. Then the averaged K may be expanded, $K(\mathbf{q},\mathbf{r}) = \sum_\ell (2\ell+1)\, K_\ell(q,p)\, P^\ell(\cos\theta)$, and a relation between the moments follows from (5)

$$C_{\mathbf{P}}^{\ell m}(q) - \delta^{\ell 0}\, \delta^{m 0} = 4\pi \int_0^\infty dr\, r^2\, K_\ell(q,r)\, S_{\mathbf{P}}^{\ell m}(r)\,. \tag{10}$$

In the proton-proton case, the $\ell = 0$ operator is

$$K_0(q,r) = \frac{1}{2} \sum_{js\ell\ell'} (2j+1)\, \left(g_{js}^{\ell\ell'}(r)\right)^2 - 1\,, \tag{11}$$

where $g_{js}^{\ell\ell'}$ is the radial wave function with outgoing asymptotic angular momentum ℓ. In the classical limit of correlations of purely Coulomb origin, such as investigated between

intermediate-mass fragments [10], the operator is $K_0(q,r) = \theta(r-r_c)\,(1-r_c/r)^{1/2} - 1$, with the distance of closest approach $r_c(q) = 2\mu\, Z_1\, Z_2\, e^2/q^2$.

In the general case, the source determination may be carried out by discretizing the functions and integrals in equations such as (1), (5), or (10), and fitting the discretized values of S. We illustrate this by analyzing the proton-proton correlation data [11,12] from the 75 MeV/nucleon ^{14}N + ^{27}Al reaction, displayed in Fig. 2.

With the data [12] averaged over the $\mathbf{q}$ directions, we concentrate on the relation (10) between the angle-averaged S and C. At high relative-momenta the assumptions leading to (1) may break down. Further, at high momentum, correlations within the source, such as associated with the ansisotropic flow [13], may play a role and, in addition, the event selection for singles in [12] becomes an issue. Thus, we restrict the region for source determination to less than $q_{\rm max} \simeq 80$ MeV/c. From below, given the issues of experimental resolution [12], we restrict the region of analysis to $q > q_{\rm min} = 10$ MeV/c. This sets a lower limit on the resolution within the source of $1/2(q_{\rm max}-q_{\rm min}) \simeq 1.4$ fm, and we settle at the determination of the source values at points separated by a coarser $\Delta r = 1.8$ fm, $r_k = (k-\frac{1}{2})\Delta r$. We represent the source function as

$$S_{\mathbf{P}}(r) \simeq \sum_k S_{\mathbf{P}}(r_k)\, g(r-r_k)\,, \tag{12}$$

where g is a profile function, $g(x) = 1$ for $|x| < \Delta r/2$, and $g(x) = 0$ otherwise. Then from (10), we get

$$C_{\mathbf{P}}(q) \simeq \sum_k w_k(q)\, S_{\mathbf{P}}(r_k)\,, \tag{13}$$

where $w_k = 4\pi \int dr\, r^2\, K_0(q,r)\, g(r-r_k)$. On determining the pp wavefunctions for $\ell, \ell' \leq 2$ from the Schrödinger equation with the regularized Reid soft-core potential [14], we finally minimize $\chi^2_{\mathbf{P}} = \sum_j ((C^{\rm exp}_{\mathbf{P}}(q_j) - C_{\mathbf{P}}(q_j))/\sigma_j)^2$ by varying $S(r_k)$, subject to the conditions that $S(r_k) \geq 0$ and that S is normalized to 1. Initially, we aimed at determining the source up to $r_{\rm max} \sim 30$ fm, but found that the fits favored S consistent with zero at the higher r within that range. We were thus able to reduce $r_{\rm max}$ for the considered spatial range to 16.2 fm, without an appreciable worsening in the fits.

The source functions extracted from the data [11,12] are shown for the three total-momentum gates in Fig. 3 together with the source functions determined directly within Boltzmann-equation reaction-simulations [15,11]. The errors on each S from the data include an uncertainty from varying $q_{\rm max}$ in the vicinity of 80 MeV/c. The values of χ^2 per degree of freedom are 1.1 for the highest momentum gate, 1.8 for the lowest, and 4.9 for the intermediate one with the lowest errors on the data.

We now discuss the relative proton functions, both for the data and the model, together with the informational content in such types of functions. The changes in the spatial relative distribution function in Fig. 3, from a compact form at high proton momenta to an extended form at low momenta, demonstrate the presence of space-momentum correlations within the ^{14}N + ^{27}Al reaction. At intermediate and low momenta, neither the relative proton distributions from the data, nor those from the model, could be well approximated by Gaussians. This is in contrast to the distribution in Fig. 1, and, to a degree, to the distributions for high momenta in Fig. 3. Overall, the transport model yields distributions in a near-quantitative agreement with the experimental sources. (The nuclear matter density is now initialized within the model by solving the Thomas-Fermi equations, unlike what was done in [11].) Only at the shortest r, the model source values seem to underestimate, systematically, the values from the data.

For a rapid freeze-out with $D(\mathbf{p},\mathbf{r},t) \simeq f(\mathbf{p},\mathbf{r})\,\delta(t-t_0)$ where f is the Wigner function, and for weak *directional* correlations between the total and relative momentum of pairs, and between the spatial and momentum variables, the momentum average of S would approximate the relative distribution of emission points for any two particles from the reaction, and not just for the particles with close momenta. Thus, the relative distribution for any two particles, given a rapid freeze-out, is

$$\mathcal{S}(\mathbf{r}) = \frac{\int d\mathbf{P}\, d\mathbf{p}\, d\mathbf{R}\, f(\mathbf{P}/2+\mathbf{p},\mathbf{R}+\mathbf{r}/2)\, f(\mathbf{P}/2-\mathbf{p},\mathbf{R}-\mathbf{r}/2)}{\int d\mathbf{p}_1\, d\mathbf{r}_1\, f(\mathbf{p}_1,\mathbf{r}_1) \int d\mathbf{p}_2\, d\mathbf{r}_2\, f(\mathbf{p}_2,\mathbf{r}_2)}. \qquad (14)$$

We now rewrite and expand the expression in the numerator in (14):

$$f(\mathbf{P}/2+\mathbf{p},\mathbf{R}+\mathbf{r}/2)\, f(\mathbf{P}/2-\mathbf{p},\mathbf{R}-\mathbf{r}/2)$$

$$= \int d\mathbf{r}_1' \, f(\mathbf{p}_1, \mathbf{r}_1') \int d\mathbf{r}_2' \, f(\mathbf{p}_2, \mathbf{r}_2') \, \frac{f(\mathbf{P}/2 + \mathbf{p}, \mathbf{R} + \mathbf{r}/2) \, f(\mathbf{P}/2 - \mathbf{p}, \mathbf{R} - \mathbf{r}/2)}{\int d\mathbf{r}_1' \, f(\mathbf{P}/2 + \mathbf{p}, \mathbf{r}_1') \int d\mathbf{r}_2' \, f(\mathbf{P}/2 - \mathbf{p}, \mathbf{r}_2')}$$

$$= \int d\mathbf{r}_1' \, f(\mathbf{p}_1, \mathbf{r}_1') \int d\mathbf{r}_2' \, f(\mathbf{p}_2, \mathbf{r}_2') \left(1 + \mathbf{p} \frac{\partial}{\partial \mathbf{p}'} + \ldots\right)$$

$$\times \left. \frac{f(\mathbf{P}/2 + \mathbf{p}', \mathbf{R} + \mathbf{r}/2) \, f(\mathbf{P}/2 - \mathbf{p}', \mathbf{R} - \mathbf{r}/2)}{\int d\mathbf{r}_1' \, f(\mathbf{P}/2 + \mathbf{p}', \mathbf{r}_1') \int d\mathbf{r}_2' \, f(\mathbf{P}/2 - \mathbf{p}', \mathbf{r}_2')} \right|_{\mathbf{p}'=0} . \tag{15}$$

The gradient term must be proportional to a combination of the vectors $\mathbf{P}$, $\mathbf{r}_1$, and $\mathbf{r}_2$ and for the weak directional correlations it would average to zero under the integration in (14). Inserting (15) into (14) and keeping the leading term, we obtain

$$\mathcal{S}(\mathbf{r}) \simeq \frac{1}{N^2} \int d\mathbf{p}_1 \, d\mathbf{p}_2 \, \frac{dN}{d\mathbf{p}_1} \, \frac{dN}{d\mathbf{p}_2} \, \gamma_P \, S_{\mathbf{P}}(\mathbf{r} + \mathbf{n}_{\mathbf{P}} \, (\gamma_P - 1)(\mathbf{n}_{\mathbf{P}} \, \mathbf{r})) \, , \tag{16}$$

where N is particle multiplicity and $\mathbf{n}_{\mathbf{P}} = \mathbf{P}/P$. The argument of $S_{\mathbf{P}}$ has been written in the cm frame of an emitted pair and γ_P is the Lorentz factor for the transformation from the system frame to the pair cm frame.

Generally, the relative distribution of emission points for any two particles, at $r \to 0$, multiplied by $N - 1$, gives an average freeze-out density. Thus, if the assumptions above are valid, this density may be obtained by multiplying the average (16) of $S_{\mathbf{P}}(r \to 0)$ by $N - 1$. The transport calculations [15] indicate that the measured [12] coincidence cross sections for the ^{14}N + ^{27}Al reaction are dominated by rather central collisions with $b \sim 2.8$ fm. Only for such collisions is there a large chance of detecting two particles at a wide angle simultaneously. The rms nucleon cm momentum in the central collisions is ~ 185 MeV/c. At 25° this corresponds to ~ 320 MeV/c nucleon laboratory momentum, or ~ 640 MeV/c total momentum for a pair. Thus, the results for the intermediate-momentum gate in Fig. 3 best represent the average situation in the central collision. Under the assumptions mentioned above, together with the presumption that the relative spatial distributions of other particles to protons is similiar to that of two protons, this relative spatial distribution yields then an average nuclear density in the vicinity of any emitted proton of $17 \times S(r \to 0) \simeq 17 \times 0.0015 \text{ fm}^{-3} = 0.025 \text{ fm}^{-3} = 0.16 \, n_0$. Here we assume the participants to have a total mass of 18 following from the fireball geometry at $b \approx 2.8$ fm. The direc-

tional space-momentum correlations anticipated in collisions due to a collective motion, to shadowing, or to emission that is most likely not instantaneous, make the obtained value actually an upper limit on the freeze-out density.

Irrespective of any correlations or of the validity of instantaneous freeze-out, the product of the $r \to 0$ source-function and the momentum distribution yields the space average of the phase-space occupancy at freeze-out,

$$\langle f \rangle(\mathbf{p}) = \frac{(2\pi)^3}{2s+1} \frac{E_p}{m} \frac{dN}{d\mathbf{p}} S_{2\mathbf{p}}(r \to 0)\,, \tag{17}$$

see also [4]. Refs. [12,11] give the inclusive proton cross-sections in the $^{14}\mathrm{N} + {}^{27}\mathrm{Al}$ reaction, but only at two angles and the cross sections include large contributions from peripheral events. Under these circumstances, one might use the thermal distribution $dN_{\mathrm{th}}/d\mathbf{p} \propto 1/(z^{-1}\,\mathrm{e}^{p^2/2mT}+1)$, for the central events, in formula (17). Here z is set from the requirement of maximum entropy. For ~ 9 participant protons at $b = 2.8$ fm in the $^{14}\mathrm{N} + {}^{27}\mathrm{Al}$ reaction, that requirement gives $z \sim 1.10$ and $T \approx 10.2$ MeV. Equation (17) can be used to determine the phase-space average of the occupancy at freeze-out, $\langle f \rangle = \int d\mathbf{p}\,(\langle f \rangle(\mathbf{p}))^2 \,/\, \int d\mathbf{p}\,\langle f \rangle(\mathbf{p})$, and to estimate the entropy per nucleon,

$$\frac{S}{A} \approx - \frac{\int d\mathbf{p}\,(\langle f \rangle(\mathbf{p})\,\log(\langle f \rangle(\mathbf{p})) - (1-\langle f \rangle(\mathbf{p}))\,\log(1-\langle f \rangle(\mathbf{p})))}{\int d\mathbf{p}\,\langle f \rangle(\mathbf{p})}\,.$$

Use of the thermal momentum distribution for the $^{14}\mathrm{N} + {}^{27}\mathrm{Al}$ reaction yields $\langle f \rangle \approx 0.23$ and $S/A \approx 2.7$. For a distribution with nonequilibrium features, these values should represent the lower limit on the average occupation and the upper limit on the entropy. Indeed, when applied to the transport model, using a thermal distribution yields an entropy about 0.5 per nucleon higher than the entropy calculated directly within the model.

We have shown how to determine the relative source functions for particles directly from correlation data. When going beyond the Gaussian fitting, direct Fourier inversion, or the plain discretization of the source, the singular value decomposition [16] might be useful. This method allows one to determine what kind of source parametrization can be practically narrowed down by the correlation data. We hope that we have extended, with our investigation, the amount of information accessible within the heavy-ion reactions.

ACKNOWLEDGMENTS

The authors thank Dariusz Miśkowiec and Peter Braun-Munzinger for providing them the pion correlation data in a numerical form. They further acknowledge the conversations with colleagues, that have planted the seeds for this work, in particular with Herbert Ströbele, George Bertsch, and Scott Pratt. Finally, the authors thank Volker Koch for reading the manuscript. This work was partially supported by the National Science Foundation under Grant PHY-9403666 and by the Department of Energy under Grant FG06-90ER40561.

REFERENCES

[1] J. T. Armstrong *et al.*, Physics Today 48, 42 (1995).

[2] D. Buscher *et al.*, Mon. Not. R. Astro. Soc. 245, 7 (1990).

[3] D. H. Boal, C. K. Gelbke, and B. K. Jennings, Rev. Mod. Phys. 62, 553 (1990).

[4] G. F. Bertsch, Phys. Rev. Lett. 72, 2349 (1994).

[5] S. Pratt, T. Csörgő, and J. Zimányi, Phys. Rev. C 42, 2646 (1990).

[6] P. Danielewicz and P. Schuck, Phys. Lett. B 274, 268 (1992).

[7] P. Danielewicz and D. Brown, in preparation.

[8] G. Baym and P. Braun-Munzinger, report nucl-th/9606055, 1996.

[9] D. Miśkowiec (E877 Collaboration), Nucl. Phys. A610 (1996).

[10] Y. D. Kim *et al.*, Phys. Rev. Lett. 67, 14 (1991).

[11] W. G. Gong *et al.*, Phys. Rev. C 47, R429 (1993).

[12] W. G. Gong *et al.*, Phys. Rev. C 43, 1804 (1991).

[13] B. Kämpfer *et al.*, Phys. Rev. C 48, R955 (1993).

[14] V. G. J. Stoks *et al.*, Phys. Rev. C 49, 2950 (1994).

[15] P. Danielewicz, Phys. Rev. C 51, 716 (1995).

[16] W. H. Press *et al.*, *Numerical Recipes* (Cambridge U. Press, Cambridge, 1986).

FIGURES

FIG. 1. Relative negative-pion source-function determined from the correlation data of Ref. [9]. Prior to the integration in Eq. (9), the relative momenta in the correlation function have been increased by 8% to correct for the Coulomb effect of the source; similar reduction of the momenta in the positive-pion correlation function brings the two correlation functions (or the source functions) into rough agreement with each other. The shaded area represents uncertainty in the source function associated with the uncertainty in the determination of the π^- correlation function [9] and due to the choice of $q_{max} \simeq 50$ MeV/c.

FIG. 2. Two-proton correlation function for the $^{14}N + ^{27}Al$ reaction at 75 MeV/nucleon. The symbols represent data [12,11] for three gates of total momentum imposed on protons emitted in the vicinity of $\theta_{lab} = 25°$. The lines represent the correlation function for the extracted sources displayed in Fig. 3.

FIG. 3. Relative source function for protons emitted from the $^{14}N + ^{27}Al$ at 75 MeV/nucleon, in the vicinity of $\theta_{lab} = 25°$, within three total momentum intervals. Filled circles represent the function extracted from the data [12,11]. Open circles represent the function determined within the Boltzmann-equation model [15].

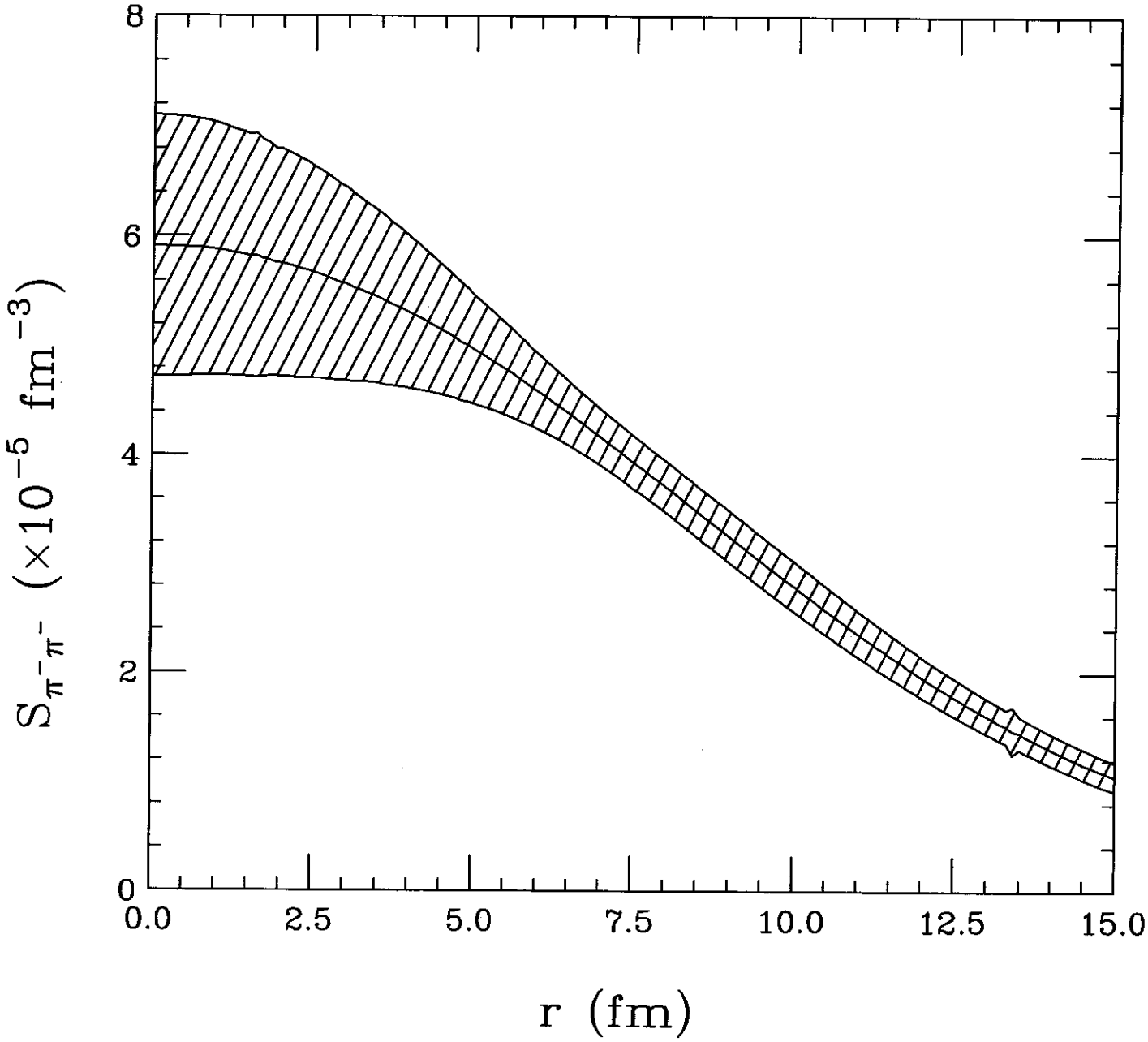

Figure 1

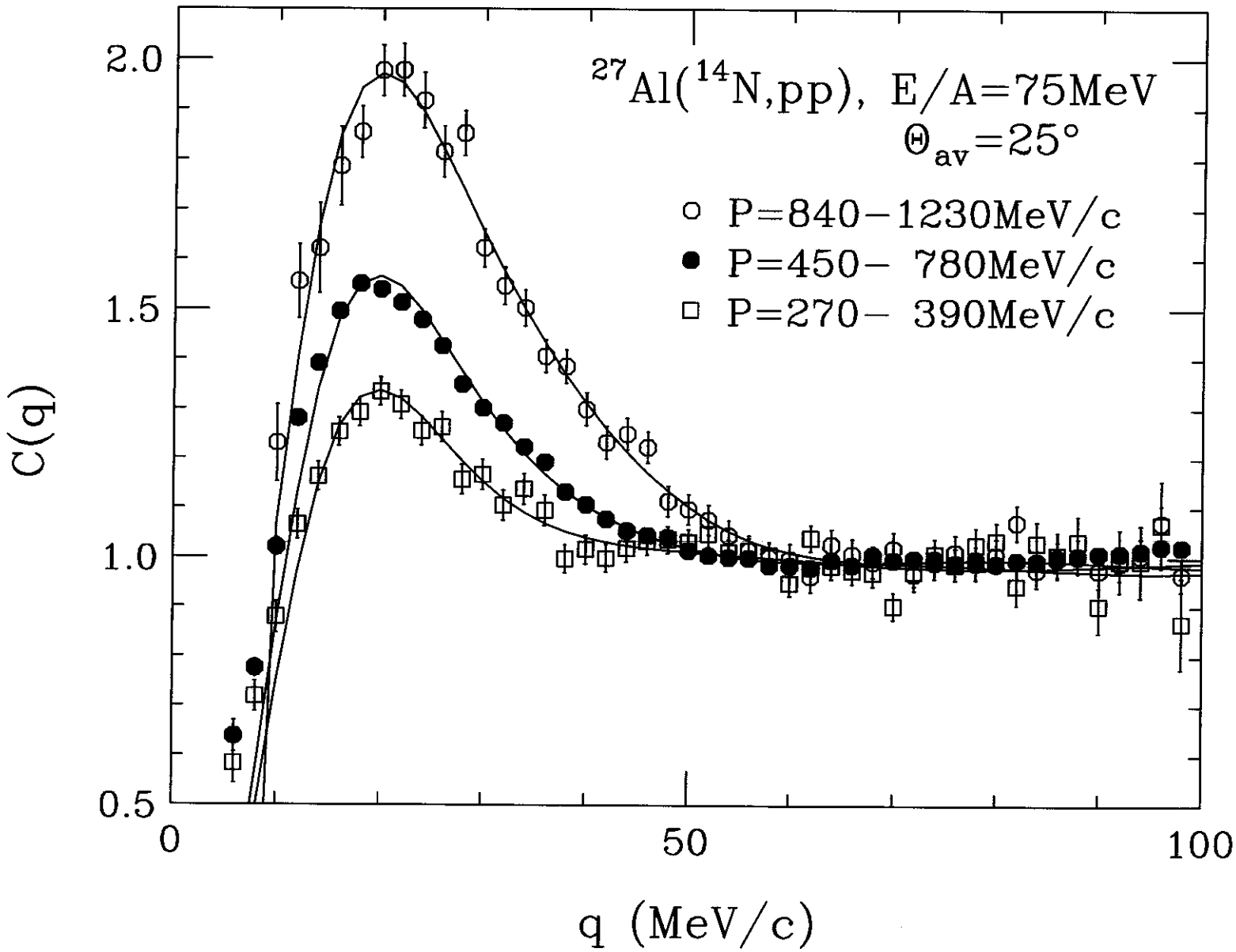
^{27}Al(^{14}N,pp), E/A=75MeV
Θ_{av}=25°
P=840−1230MeV/c
P=450− 780MeV/c
P=270− 390MeV/c
C(q)
q (MeV/c)
2.0
1.5
1.0
0.5
0
50
100

Figure 2

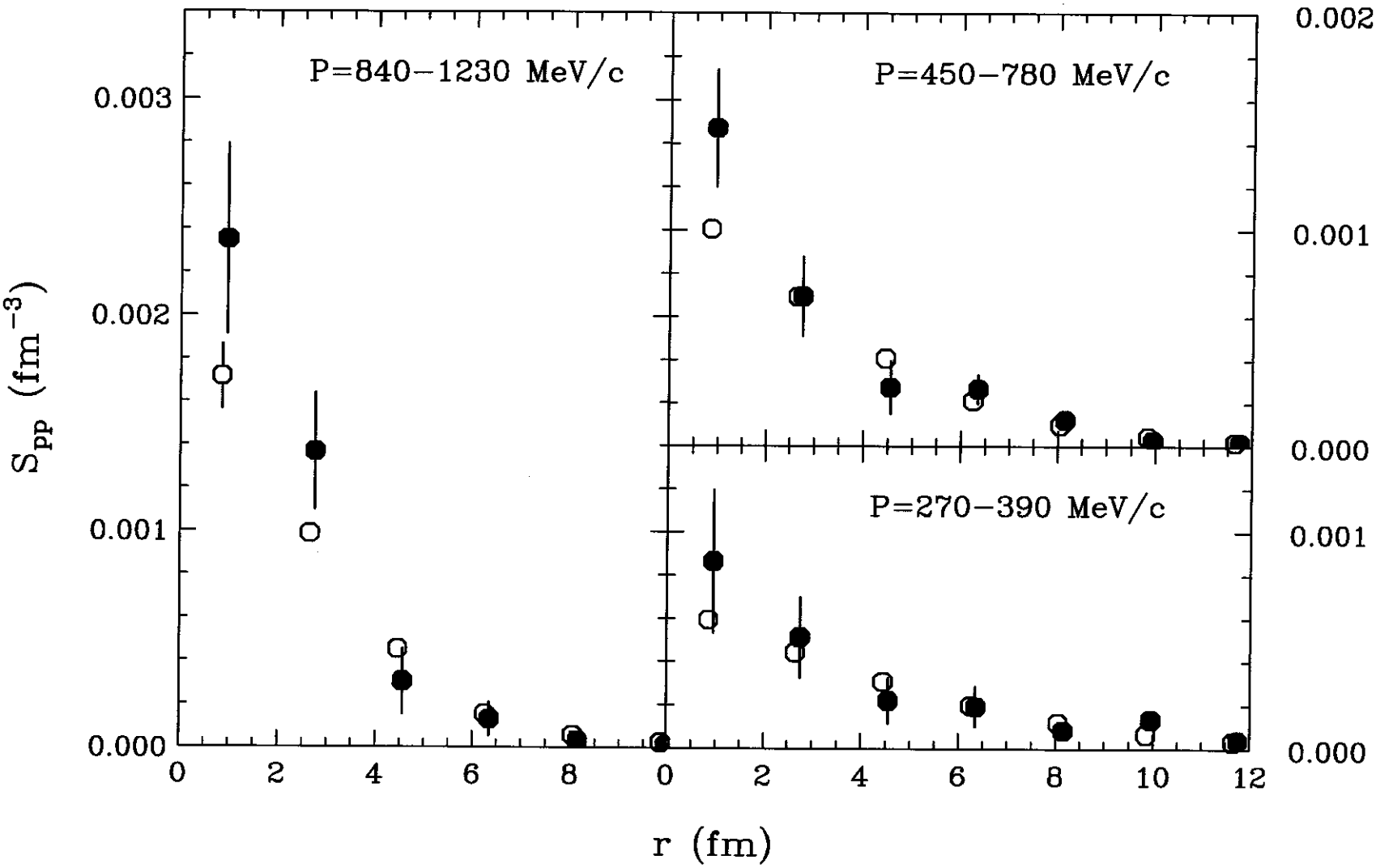
P=840−1230 MeV/c
P=450−780 MeV/c
P=270−390 MeV/c
S_{pp} (fm^{-3})
r (fm)
0.000
0.001
0.002
0.003
0
2
4
6
8
10
12

Figure 3